Measuring Soil Water Content with Ground Penetrating Radar: A Review

J. A. Huisman,* S. S. Hubbard, J. D. Redman, and A. P. Annan

ABSTRACT

We present a comprehensive review of methods to measure soil water content with ground penetrating radar (GPR). We distinguish four methodologies: soil water content determined from reflected wave velocity, soil water content determined from ground wave velocity, soil water content determined from transmitted wave velocity between boreholes, and soil water content determined from the surface reflection coefficient. For each of these four methodologies, we discuss the basic principles, illustrate the quality of the data with field examples, discuss the possibilities and limitations, and identify areas where future research is required. We hope that this review will further stimulate the community to consider ground penetrating radar as one of the possible tools to measure soil water content.

WATER AT THE LAND SURFACE is a vital resource for both human needs and natural ecosystems. Society's fresh water needs for agriculture, sanitation, municipal, and industrial supply are ever increasing. At the same time, natural hazards involving water, such as floods, droughts and landslides are major natural threats to society in many countries (Entekhabi et al., 1999). The vadose zone, which may be defined as the transition zone between the atmosphere and groundwater reservoirs, is important for water resource management, because it regulates the water availability for vegetation, including crops, while at the same time provides a protective buffer zone between land surface and groundwater against solutes and pollutants (Rubin, 2003).

Hydrologists, soil scientists, ecologists, meteorologists, and agronomists all study the space and time variability of water in the vadose zone, hereafter referred to as soil water content, over a range of scales and for a variety of reasons. At the regional to continental scale, the exchange of moisture and energy between soil, vegetation, and the atmosphere has an impact on near-surface atmospheric moisture and temperature, which in turn define the regional climate. For example, soil water content determines to a large extent the relative magnitudes of sensible and latent heat fluxes and therefore determines the diurnal evolution of the atmospheric boundary layer (Callies et al., 1998). Currently, there is a need to establish and quantify the contribution of soil water content–regulated land–atmosphere coupling to regional climate anomalies, such as continental droughts and large-scale precipitation events (Entekhabi et al., 1999).

At the catchment scale, soil water content partly controls the separation of precipitation into infiltration, evaporation, and runoff and therefore has a large influence on soil erosion and river discharge. Recent studies have shown that including soil water content heterogeneity in spatially distributed hydrological models can improve discharge predictions (Merz and Plate, 1997; Merz and Bardossy, 1998; Pauwels et al., 2001). However, there is no consensus on how to incorporate spatial soil water content heterogeneity in these models. Some have suggested that it is sufficient to include the statistics (spatial mean and variance) of measured soil water content structure (e.g., Pauwels et al., 2001), whereas others have suggested that discharge predictions also improve when a full description of soil water content variation is included (Merz and Bardossy, 1998). Furthermore, Merz and Plate (1997) argued that the improvement of discharge predictions by including soil water content heterogeneity will strongly depend on the event characteristics, including antecedent soil water conditions and rainfall intensities.

At the field scale, information on the spatial distribution of soil water is important for precision agriculture programs. With too much water, crop quality could decrease due to the adverse effects of waterlogged plant roots (e.g., reduced root respiration due to depletion of O_2 and increased availability of toxic ions under reducing soil conditions). With too little water, crops can be irreversibly damaged due to drought stress. In addition to the impact of water content on the quality and quantity of crops, the outlay of resources and energy concomitant with crop irrigation is critical in water-scarce regions, especially as competition for water resources between rural and agricultural land users increases.

Clearly there is a need for soil water content measurements across a range of spatial scales. High-frequency electromagnetic techniques are the most promising category of soil water content sensors to fulfill this need because this category contains a range of techniques that measure the same soil water content proxy, namely dielectric permittivity, at different spatial scales. Remote sensing with either passive microwave radiometry or active radar instruments is the most promising technique for measuring soil water content variations over

J.A. Huisman, Center for Geo-Ecological Research (ICG), Institute for Biodiversity and Ecosystem Dynamics (IBED)– Physical Geography, Universiteit van Amsterdam, The Netherlands (currently Dep. of Landscape Ecology and Resources Management, Justus-Liebig-University Giessen, Heinrich-Buff-Ring 26-32, 35372 Giessen, Germany); S.S. Hubbard, Lawrence Berkeley National Laboratory and University of California, Berkeley, CA; J.D. Redman and A.P. Annan, Sensors and Software Inc., Mississauga, ON, Canada. Received 13 Mar. 2003. Special Section—Advances in Measurement and Monitoring Methods. *Corresponding author (sander.huisman@agrar.uni-giessen.de).

Abbreviations: CMP, Common-MidPoint; CPT, cone penetrometer; GPR, ground penetrating radar; MOP, multi-offset profile; SWC, soil water content; TDR, time domain reflectometry; VRP, vertical radar profiling; WARR, Wide Angle Reflection and Refraction; ZOP, zero offset profile.

large regions (Jackson et al., 1996; Ulaby et al., 1996, Famiglietti et al., 1999; van Oevelen, 2000). The passive instruments have low spatial resolution and can either be airborne with pixel sizes of thousands of square meters or satellite-borne with footprints in the order of tens of square kilometers. In the near future, passive satellite remote sensing will provide global coverage of critical hydrological data, including soil water content (Entekhabi et al., 1999). Active radar instruments have smaller pixel sizes ranging from 1 to several 1000 m^2. Although remote sensing will surely play an important role in many future hydrological studies, currently there is still a need to establish transfer functions between remote sensing and the more familiar in situ soil water content measurements. Additionally, because remote sensing approaches for estimating water content estimate water content in the uppermost 0.05 m of the soil and require that the vegetation cover is minimal (Jackson et al., 1996), remote sensing methods are not applicable in all types of vadose zone studies.

A well-established in situ electromagnetic technique for soil water content investigations is time domain reflectometry (TDR), which was introduced in vadose zone hydrology in the early 1980s (Topp et al., 1980). Time domain reflectometry has developed into a reliable method for soil water content determination that can easily be automated (Heimovaara and Bouten, 1990). Furthermore, TDR can simultaneously measure dielectric permittivity and bulk soil conductivity (Dalton et al., 1984; Topp et al., 1988), which allows the study of water and solute transport within the same soil volume. Although TDR is highly suited for monitoring the development of soil water content at one location with a high temporal resolution, the small measurement volume ($<$dm^3) makes it sensitive to small-scale soil water content variation (e.g., macropores, air gaps due to TDR insertion) within this volume (Ferré et al., 1996). Furthermore, assessment of spatial soil water content variation with TDR is labor intensive because TDR sensors need to be installed at each measurement location.

Clearly, there is a scale gap between remote sensing and TDR measurements of soil water content. At intermediate spatial scales, such as agricultural land and small catchments, reliance on sparse TDR measurements or coarse remote sensing measurements might not provide the accurate soil water content information required at these scales (e.g., crop management, precision farming). Therefore, there is a need for soil water content measurement techniques that can provide dense and accurate measurements at an intermediate scale. Since the early days of electromagnetic measurement techniques, ground penetrating radar (GPR) has been conceived as the natural intermediate-scale counterpart of TDR for soil water content measurements. Although the number of TDR applications has increased immensely in the past 20 yr, the number of GPR applications for measuring soil water content has only recently increased. Probably, the most important reason behind this delay is the more complicated behavior of the unguided waves used in GPR as compared with waves guided by a TDR sensor. Furthermore, recent improvements in GPR technology

allow more accurate travel time measurements, which are needed for soil water content determination with GPR. In this review, we present an overview of the available methods for estimating soil water content with GPR. Additionally, we discuss the possibilities and limitations of each of the methods. Hopefully, this review will further stimulate readers to consider GPR as one of the viable options for soil water content determination.

PRINCIPLES OF ELECTROMAGNETIC METHODS
Electromagnetic Wave Propagation

The propagation velocity of electromagnetic waves, v (m s^{-1}), is determined by the complex dielectric permittivity, $\varepsilon^*(f) = \varepsilon'(f) - j\varepsilon''(f)$

$$v(f) = \frac{c}{\sqrt{\varepsilon'(f)\mu_r \dfrac{1 + \sqrt{1 + \tan^2 \delta}}{2}}} \qquad [1]$$

with the loss tangent δ defined as

$$\tan \delta = \frac{\varepsilon''(f) + \dfrac{\sigma_{dc}}{2\pi f \varepsilon_0}}{\varepsilon'(f)} \qquad [2]$$

and where c is free space electromagnetic propagation velocity (3×10^8 m s^{-1}), f is the frequency of the electromagnetic field (Hz), $\varepsilon'(f)$ is the real part of the relative dielectric permittivity, $\varepsilon''(f)$ is the imaginary part of the relative dielectric permittivity, μ_r is the relative magnetic permeability, σ_{dc} is the DC conductivity (S m^{-1}), and ε_0 is the free space permittivity (8.854×10^{-12} F m^{-1}). For nonmagnetic soils, μ_r equals 1 in the GPR frequency range (van Dam et al., 2002). Throughout this review, permittivity is understood to represent the relative dielectric permittivity, ε_r, that is, the permittivity relative to free space as calculated by the absolute permittivity, ε (F m^{-1}), divided by the free space permittivity ε_0 (F m^{-1}):

$$\varepsilon_r = \frac{\varepsilon}{\varepsilon_0} \qquad [3]$$

The imaginary part of the permittivity, $\varepsilon''(f)$, is associated with the energy dissipation, and the real part of the permittivity, $\varepsilon'(f)$, is associated with the capability to store energy when an alternating electrical field is applied. The complex permittivity of most materials varies considerably with the frequency of the applied electric field. An important process contributing to the frequency dependence of permittivity is the polarization arising from the orientation with the imposed electric field of molecules that have permanent dipole moments. The mathematical formulation of Debye describes this process for pure polar materials (Debye, 1929):

$$\varepsilon^*(f) = \varepsilon_\infty + \frac{\varepsilon_s - \varepsilon_\infty}{1 + \left(i \dfrac{f}{f_{rel}}\right)} - \frac{j\sigma_{dc}}{2\pi f \varepsilon_0} \qquad [4]$$

where ε_∞ represents the permittivity at frequencies so high that molecular orientation does not have time to contribute to the polarization, ε_s represents the static permittivity (i.e., the value at zero frequency), and f_{rel} (Hz) is the relaxation frequency, defined as the frequency at which the permittivity equals $(\varepsilon_s + \varepsilon_\infty)/2$ (Nelson, 1994). The separation of Eq. [4]
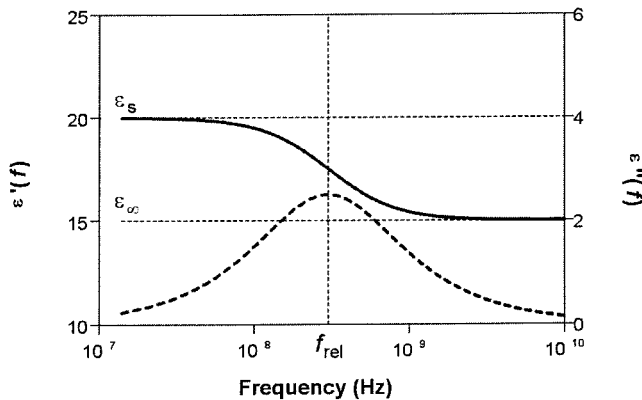
Fig. 1. Example of the Debye model for the real part (solid line) and imaginary part (dashed line) of the permittivity.

into its real and imaginary part is shown in Fig. 1 for an idealized medium with $\varepsilon_s = 20$, $\varepsilon_\infty = 15$, $f_{rel} = 10^{8.47}$ Hz (300 MHz) and $\sigma_{dc} = 0$ S m^{-1}. Figure 1 shows that at frequencies very low and very high with respect to relaxation processes, the permittivity has constant values and zero losses. At intermediate frequencies, the permittivity undergoes a dispersion, and dielectric losses occur with the peak loss at $f = f_{rel}$. Water in its liquid state is a prime example of a polar dielectric. The Debye parameters of water are $\varepsilon_s = 80.1$, $\varepsilon_\infty = 4.2$, and $f_{rel} = 10^{10.2}$ Hz (17.1 GHz) at 25°C (Hasted, 1973). In sandy soils, most water is effectively in its free liquid state. In high clay content soils, pore water is not necessarily in its free liquid state. Sometimes it is physically absorbed in capillaries, limited in motion by electrostatic interaction with clay particles. Dielectric relaxation of absorbed water takes place at lower frequencies than the relaxation of free water (Hasted, 1973; Or and Wraith, 1999).

In the case of GPR measurements, which commonly have a frequency bandwidth from 10 MHz to 1 GHz, $\varepsilon''(f)$ is often small compared with $\varepsilon'(f)$. Furthermore, many soils do not show relaxation of permittivity in the frequency range of 10 MHz to 1 GHz. Under these conditions, Eq. [1] reduces to

$$v = \frac{c}{\sqrt{\varepsilon'}} \qquad [5]$$

for nonsaline soils (Wyseure et al., 1997). The real part of the permittivity of water within the megahertz to gigahertz bandwidth is approximately 80, whereas the permittivity of air is 1 and of most other common soil constituents is about 3 to 10. This large contrast in permittivity explains the success of soil water content measurements with electromagnetic techniques working within this frequency bandwidth.

Water Content–Permittivity Relationships

The most commonly used relationship between apparent permittivity, ε, and volumetric soil water content, θ (m^3 m^{-3}), was proposed by Topp et al. (1980):

$$\theta = -5.3 \times 10^{-2} + 2.92 \times 10^{-2}\,\varepsilon - 5.5 \times 10^{-4}\,\varepsilon^2$$
$$+\ 4.3 \times 10^{-6}\,\varepsilon^3 \qquad [6]$$

and was determined empirically for mineral soils having various textures. It has an accuracy of 0.022 m^3 m^{-3} determined in an independent validation on mineral soils (Jacobsen and Schjønning, 1994). The term *apparent* is used because the permittivity used in this equation is determined from the measured electromagnetic propagation velocity in the soil.

A more theoretical approach to relating soil water content

and ε is based on dielectric mixing models, which use the volume fractions and the dielectric permittivity of each soil constituent to derive a relationship (e.g., Dobson et al., 1985; Roth et al., 1990; Friedman, 1998; Jones and Friedman, 2000). In dielectric mixing models, the bulk permittivity of a soil–water–air system, ε_b, may be expressed with the Complex Refractive Index Model (CRIM):

$$\varepsilon_b = \left[\theta\varepsilon_w^\alpha + (1-n)\varepsilon_s^\alpha + (n-\theta)\varepsilon_a^\alpha\right]^{\frac{1}{\alpha}} \qquad [7]$$

where n (m^3 m^{-3}) is the soil porosity; ε_w, ε_s, and ε_a are the permittivities of water, soil particles and air, respectively; and α is a factor accounting for the orientation of the electrical field with respect to the geometry of the medium ($\alpha = 1$ for an electrical field parallel to soil layers, $\alpha = -1$ for an electrical field perpendicular to soil layers, and $\alpha = 0.5$ for an isotropic medium). After rearranging Eq. [7], the following expression can be obtained for soil water content:

$$\theta = \frac{\varepsilon_b^\alpha - (1-n)\varepsilon_s^\alpha - n\varepsilon_a^\alpha}{\varepsilon_w^\alpha - \varepsilon_a^\alpha} \qquad [8]$$

After substitution of $\varepsilon_a = 1$ and assuming $\alpha = 0.5$, Eq. [8] reduces to

$$\theta = \frac{1}{\sqrt{\varepsilon_w} - 1}\sqrt{\varepsilon_b} - \frac{(1-n)\sqrt{\varepsilon_s} - n}{\sqrt{\varepsilon_w} - 1} \qquad [9]$$

which gives a physical interpretation of a simple soil water content–ε relationship suggested by Ledieu et al. (1986) and Herkelrath et al. (1991):

$$\theta = a\,\sqrt{\varepsilon_b} - b \qquad [10]$$

where a and b are calibration parameters and $\sqrt{\varepsilon_b}$ is also referred to as refractive index (n_a). This relationship has an accuracy of 0.0188 m^3 m^{-3}, as determined by an independent validation on mineral soils (Jacobsen and Schjønning, 1994). For more information, the reader is referred to Robinson et al. (2003) and the references therein.

It is important to realize that most available calibration equations between permittivity and water content were derived using TDR, which mainly operates in the frequency range from 500 to 1000 MHz (see Robinson et al. 2003). However, it has long been recognized that high clay content soils exhibit significant permittivity dispersion at low frequencies (e.g., Olhoeft, 1987). Recently, West et al. (2003) presented frequency-dependent permittivity measurements of fine-grained sandstone samples containing up to 5% clay and soil samples containing Ottawa sand and varying amounts of montmorillonite clay. Their result showed that both the sandstone and soil samples showed a significant frequency dispersion below 350 MHz. This implies that site-specific calibration may be required for those applications that require accurate water content measurements with lower antenna frequencies, such as the commonly used 100-MHz antenna. Clearly, this is an important research topic for the near feature. However, even when using published petrophysical relationships derived with TDR (such as Eq. [6]) with permittivity values obtained from GPR data, reasonable information about water content variation and spatial patterns can be obtained, as will be shown below.

PRINCIPLES OF GROUND PENETRATING RADAR

Ground penetrating radar is a geophysical measurement technique that has been extensively used to noninvasively map subsurface features at scales from kilometers for geologic fea-
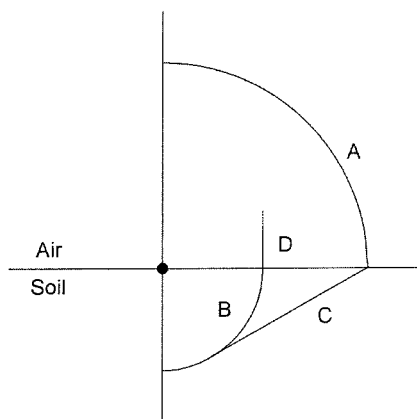
Fig. 2. Wave fronts around a dipole source on the soil surface. A and B are spherical waves in the air and soil, respectively. Wave C is the lateral or head wave in the soil, and D is the ground wave in the air (after Annan, 1973).

Fig. 3. Propagation paths of electromagnetic waves in a soil with two layers of contrasting dielectric permittivity (ε_1 and ε_2) (after Sperl, 1999).

tures to centimeters for rebar in concrete structures. Extensive literature describing GPR applications is available. An excellent introduction to GPR in hydrogeological applications is available in Davis and Annan (1989).

The GPR technique is similar in principle to seismic and sonar methods. In the case of the most commonly used bistatic systems, one antenna, the transmitter, radiates short pulses of high-frequency (MHz to GHz) electromagnetic waves, and the other antenna, the receiver, measures the signal from the transmitter as a function of time. When the source antenna is placed on the surface, spherical waves are radiated both upward into the air and downward into the soil as indicated by wave fronts A and B in Fig. 2. Because of the continuity requirements for the electromagnetic field at the soil surface, the propagating spherical air wave (A in Fig. 2) gives rise to a lateral wave front (C in Fig. 2) in the soil. Similarly, the spherical wave propagating in the soil gives rise to the ground wave (D in Fig. 2). The ground wave amplitude is known to decrease strongly with distance above the soil surface, and therefore the ground wave is not presented as a wave front in Fig. 2.

Two important aspects of GPR are resolution and depth penetration. GPR resolution is determined by the period of the emitted pulse, which is controlled by the frequency bandwidth of the GPR system. Because impulse radar systems are designed to achieve bandwidths that are about equal to the center frequency, the resolution of GPR increases with increasing center frequency (Davis and Annan, 1989). Depth penetration of GPR measurements is strongly controlled by the soil electrical conductivity combined with the center frequency of the GPR system. In low-conductivity media, such as dry sand and gravel, low-frequency GPR systems (e.g., 50- or 100-MHz antennas) can achieve penetration up to several tens of meters, and high-frequency systems (e.g., 450- or 900-MHz antennas) achieve penetration of one to several meters. For silty sands and clays, depth penetration will be significantly less. It is important to realize that this high sensitivity to soil texture and electrical conductivity reduces the range of soils where GPR can successfully be applied.

Figure 3 presents possible propagation paths for surface GPR energy. Principally, all these waves can be used to measure soil water content. In the following section, we focus on soil water content estimation using reflected and ground wave travel time data. In addition, we also discuss the estimation of water content using borehole GPR travel time data and using ground surface reflection amplitude data.
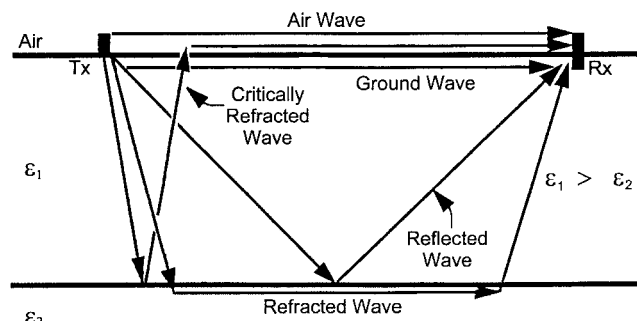
MEASURING SOIL WATER CONTENT WITH GPR

Soil Water Content Measurements with Reflected Waves

Two classes of methods to estimate soil water content from reflected wave travel time data can be distinguished. The first class contains the methods that use a single antenna separation for soil water content estimation (e.g., soil water content estimation from scattering objects and traditional GPR sections). The second class contains the methods that require multiple measurements with different antenna separations.

Single (or Common) Offset Reflection Methods

The energy that GPR transmits into the soil will be (partly) reflected when contrasts in soil permittivity are encountered. Figure 4 (right) shows an idealized GPR section measured with surface radar and a fixed antenna separation (single offset) over an anomaly (e.g., a water-filled pipe) having a different permittivity than the host material as shown in Fig. 4 (left). Because GPR emits waves in all directions, reflected energy is measured before the GPR is directly over it (Fig. 4, left). The reflected events in the radar section trace out a hyperbola (B in Fig. 4, right) because the reflected energy of the GPR measurement directly above the anomaly has the shortest travel distance (time) and all other waves will have a larger distance to travel. The average wave velocity in the soil determines the convexity of the reflection hyperbola B; i.e., it determines how much longer the waves need to travel the extra distance. The average velocity between the ground surface and the anomaly, v_{soil}, can be determined from a GPR transect by fitting the following hyperbola to measured arrival times at several positions x

$$v_{soil} = \frac{2\sqrt{x^2 + d^2}}{t_{rw,x}} \quad [11]$$

where x is the position relative to the position of the scattering object (apex of the hyperbola), d is the depth of the scattering object, and $t_{rw,x}$ is the arrival time of the reflected wave at position x that has been zero time corrected. If the GPR section is measured with a significant antenna separation, a, this should also be included in the velocity determination as follows:

$$v_{soil} = \frac{\sqrt{(x - 0.5a)^2 + d^2} + \sqrt{(x + 0.5a)^2 + d^2}}{t_{rw,x}} \quad [12]$$

Most common GPR analysis software provides routines where the velocity can be determined interactively by manually fitting hyperbola to the limbs of the reflections of the
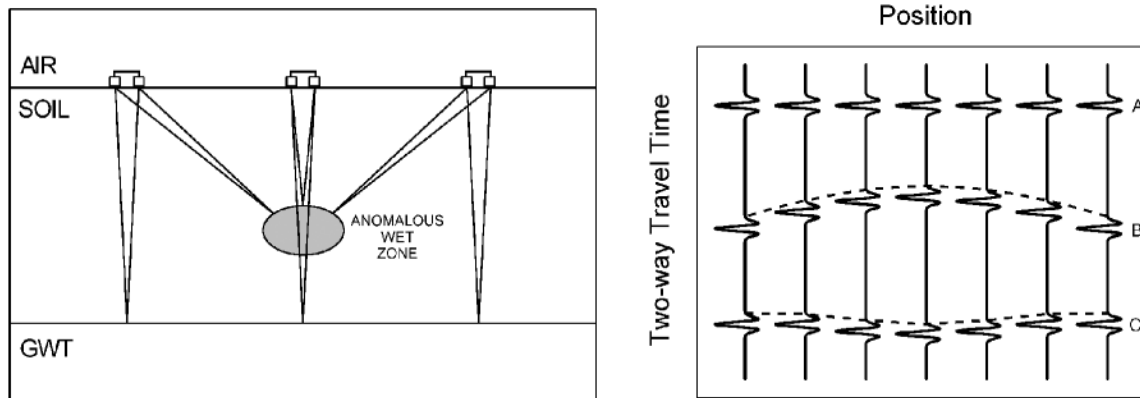
Fig. 4. Idealized ground penetrating radar (GPR) transect measured with a fixed antenna separation over an anomalous wetter zone and a horizontal groundwater table (GWT). A marks the air wave, B marks the point reflector, and C marks the reflection from the groundwater table (after Davis and Annan, 1989).

scattering object. The velocity can then be used to calculate soil permittivity (Eq. [5]) and soil water content (e.g., Eq. [6]).

The zero time correction of arrival times is required to correct for the additional travel time at the beginning of each measurement, which is mainly due to the travel time in the cables of the radar system. A commonly used correction procedure consists of (i) aligning the arrival times of the air wave to correct for drift in the zero time (e.g., caused by temperature changes affecting the radar system and the cables), (ii) estimating the average arrival time of the air wave, and (iii) calculating the zero time correction from the average arrival time and the known antenna separation. It should be noted that the methods presented in this review have different requirements for the accuracy of the zero time correction. The accuracy of borehole GPR and single offset ground wave data depends on accurate zero time corrections, whereas the accuracy of multi-offset measurements does not depend strongly on accurate zero time corrections.

Although it is simple and straightforward to determine velocity from scattering objects, it is a method that has not been used often for soil water content determination. The main drawback of this method is that it can only be used in soils where scattering objects can be observed in the GPR section. Even when scattering objects are present, this method only provides the average soil water content to the depth of the reflector; that is, the user has no control over the depth resolution of the soil water content measurements. An early application was presented by Vellidis et al. (1990), who used a reflection from a buried pipe to determine the average velocity above the wetting front, which allowed the monitoring of wetting front movement by assuming a homogeneous soil water content distribution above the wetting front.

The reflection from the top of the saturated zone, just above the groundwater table, is an example of a (semi-)horizontal contrast in soil permittivity (marked with C in Fig. 4, right). It can be seen that the anomalous wetter zone results in a pull-down of the arrival time of the wave reflected from the horizontal groundwater table because the average wave velocity to the groundwater table is lower for GPR measurements recorded above the anomaly. Unfortunately, the groundwater table reflection in a single offset measurement cannot be used to calculate the v_{soil} without knowledge of the water table depth. Of course, the water table depth (or depth of any other reflector) can be determined independently, and in such cases the arrival time of the water table reflection can easily be converted to average soil water content of the vadose zone with

$$v_{soil} = \frac{2d}{t_{rw}} \quad [13]$$

where t_{rw} is the two-way travel time of the reflected wave that has been zero time corrected and d is the water table depth. When antenna separation is significant, this equation becomes

$$v_{soil} = \frac{2\sqrt{d^2 + (0.5a)^2}}{t_{rw}} \quad [14]$$

To be useful for estimating water content, the single offset GPR reflection method requires sufficient signal penetration, the presence of a subsurface dielectric contrast that yields a clear (and preferably continuous) GPR reflector, and good control on the depth of the reflector. Shallow studies using this technique have been successfully performed using buried reflectors and engineered materials, where the depth to the reflector is well constrained. Grote et al. (2002) used the reflection travel time associated with shallow (<1 m) reflectors buried within a constructed sandy test pit to estimate water content values. Their estimates were within 0.01 m³ m⁻³ of the measured values obtained using gravimetric techniques. Grote et al. (2002) also used 1.2-GHz time-lapse single offset GPR reflection data to monitor water infiltration conducted within a pavement section consisting of permeable aggregate base layers overlain by concrete, all having a prescribed thickness. Under these engineered conditions, they obtained estimates of volumetric water content within the permeable layers as a function of depth using the GPR reflection method, which agreed with measurements obtained using gravimetric techniques to within 0.01 m³ m⁻³. Stoffregen et al. (2002) estimated volumetric water content seasonally using 1-GHz GPR reflections from the base of a 1.5-m-deep lysimeter, which was filled with sandy soils. They found that the standard deviation between the GPR estimates and the lysimeter measurements of water content was on average 0.01 m³ m⁻³ and that the estimated changes in water content corresponded with seasonal moisture variations.

The accuracy of the single offset GPR reflection method for estimating water content under natural conditions is not yet well established. Some researchers have tested the concept of using GPR reflections under natural conditions to estimate water content using depth measurements to the reflectors obtained at discrete locations from, for example, noting lithologic transitions during drilling (Weiler et al., 1998) or water table observations (van Overmeeren et al., 1997). The use of single offset GPR reflection data for estimating spatially variable
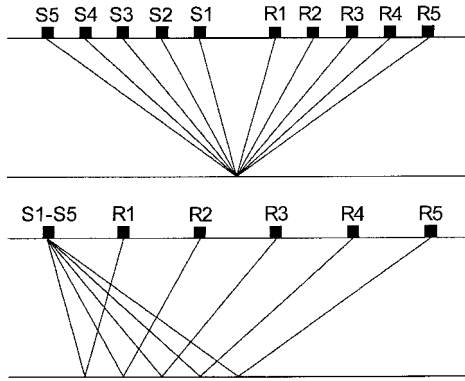
Fig. 5. Common-midpoint (CMP, top) and wide angle reflection and refraction (WARR, bottom) acquisition, where S denotes the transmitter location and R denotes the receiver locations.

water content under naturally heterogeneous conditions at the field scale is a topic of active research.

Multi-Offset Reflection Methods

Single offset measurements cannot be used to determine water content from reflecting soil layers if no information about the depth of the reflector is available. In that case, one can use a multi-offset GPR acquisition geometry to determine soil water content from radar reflections. Two commonly used multi-offset GPR acquisition geometries are called Common-MidPoint (CMP) and Wide Angle Reflection and Refraction (WARR) measurements (Fig. 5). In CMP acquisition, the distance between the antennas is increased stepwise while keeping a common midpoint. In WARR acquisition, the distance between the antennas is increased stepwise with the transmitter at a fixed position. A schematic outcome of a multi-offset GPR measurement is given in Fig. 6. If consistent reflected waves are present in the multi-offset GPR measurement, they can be used to calculate soil water content directly by fitting

$$v_{\text{soil}} = \frac{2\sqrt{d^2 + (0.5a)^2}}{t_{\text{rw,a}}} \quad [15]$$

to the zero time corrected arrival times of the reflected wave, $t_{\text{rw,a}}$, for different antenna separations, a, and solving for depth, d, and the average velocity to the reflecting layer, v_{soil} (Tillard
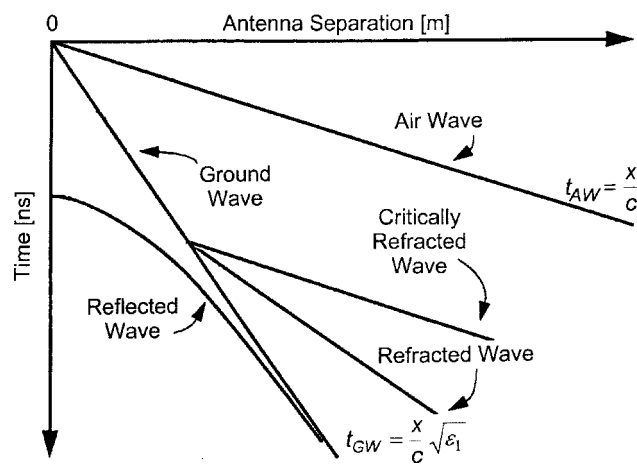
Fig. 6. Schematic wide angle reflection and refraction (WARR) measurement. The ground wave can be identified as a wave with a linear move out starting from the origin of the x–t plot. In the slope equations, c is the electromagnetic velocity in air and x is the antenna separation (after Sperl, 1999).
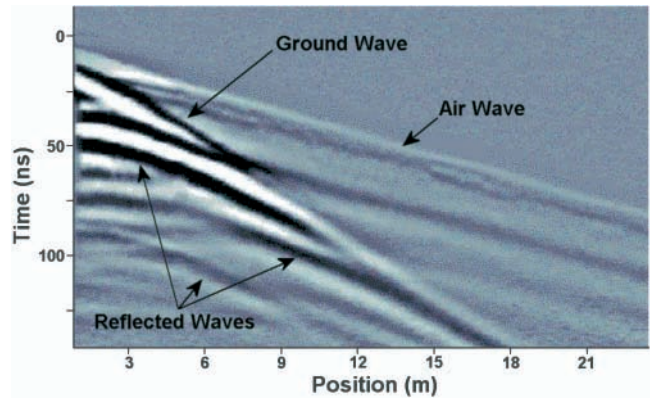
Fig. 7. Common-midpoint (CMP) measurement made with a 100-MHz antenna at the Cambridge Research Station, University of Guelph, ON, Canada.

and Dubois, 1995). Most common GPR analysis software provides routines where the velocity can be determined by manually fitting hyperbola to the reflected waves in the multi-offset measurements. Multi-offset measurements also permit velocity determination from arrivals other than the reflected waves. For example, Bohidar and Hermance (2002) showed how to use critically refracted air waves and subsurface refracted waves for soil water content determination.

To avoid subjective soil water content estimates and to speed up the analysis, (semi-)automated approaches for velocity determination from reflected GPR waves have been developed that are analogous to the velocity analysis approaches developed for use with seismic data (e.g., Yilmaz, 1987). A well-known method is semblance analysis. The aim of semblance analysis is to find the velocity and travel time for which the reflection energy of a reflected wave in a multi-offset measurement collapses to a point. This is done with help of the semblance plot, which is constructed by recalculating the arrival times of the CMP for a range of velocities (x axis of semblance plot) and summing the normalized energy for each arrival time (y axis) for each velocity. High values in the semblance plot indicate that the reflected waves at that particular arrival time are well described by that particular velocity.

The manually or semiautomatically determined velocities from the multi-offset measurement are average velocities to the depth of the reflector. To convert these average velocities to interval velocities of each layer, $v_{\text{int,n}}$, the Dix formula (Dix, 1955; Yilmaz, 1987) can be used:

$$v_{\text{int,n}} = \sqrt{\frac{t_{\text{rw,n}}v_{\text{soil,n}}^2 - t_{\text{rw,n}-1}v_{\text{soil,n}-1}^2}{t_{\text{rw,n}} - t_{\text{rw,n}-1}}} \quad [16]$$

where $v_{\text{soil,n}}$ is the average velocity from the surface down to the bottom of layer n, $v_{\text{soil,n}-1}$ is the average velocity down to the bottom of layer $n-1$, $t_{\text{rw,n}}$ is the two-way travel time to the bottom of layer n, $t_{\text{rw,n}-1}$ is the two-way travel time to the bottom of layer $n-1$, and $n=1$ is the upper layer of the soil.

The requirements for useful water content estimates with the multi-offset GPR reflection method are similar to those of single offset measurements: decent signal penetration and the presence of subsurface dielectric contrasts that yield clear (and preferably continuous) GPR reflectors. There are numerous applications of multi-offset measurements for soil water content determination (e.g., Tillard and Dubois, 1995; Greaves et al., 1996; van Overmeeren et al., 1997; Dannowski and Yaramanci, 1999; Endres et al., 2000; Nakashima et al., 2001; Bohidar and Hermance, 2002; Garambois et al., 2002). Figure 7 shows a CMP measurement made with 100-MHz antennas at the Cambridge Research Station (University of Guelph, ON,
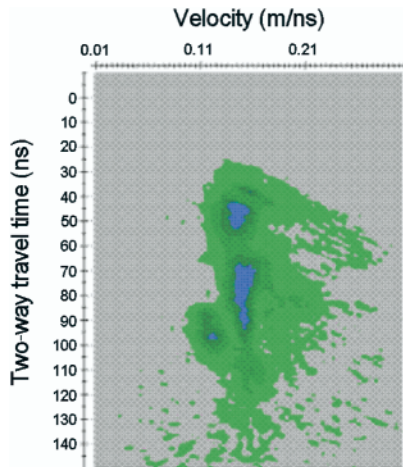
Fig. 8. Semblance plot of the common-midpoint (CMP) measurement shown in Fig. 7 to illustrate automatic extraction of velocity vs. time. Blue colors indicate a high semblance.

Fig. 9. Wide angle reflection and refraction (WARR) measurement recorded on loamy sand with the 225-MHz antennas. The velocity of the ground wave is v and of the air wave is c, both in meters per nanosecond.

Canada). The air wave, ground wave, and several reflected waves can clearly be recognized. Figure 8 presents the corresponding semblance analysis plot. The semblance analysis shows that the strong first reflection starting at about 35 ns in Fig. 7 corresponds with a velocity of about 0.13 m ns^{-1} for the upper soil layer. The second reflected wave starts at approximately 65 ns, and the semblance plot indicates that the average velocity is somewhat higher at 0.14 m ns^{-1}. Inserting these average velocities into Eq. [16] results in an interval velocity of 0.15 m ns^{-1} for the second layer. Figure 8 also shows that semblance analysis does not result in very accurate velocity estimates. The width of the velocity spectrum in Fig. 8 indicates an accuracy of about 0.02 m ns^{-1} for the velocity estimate, which translates to an accuracy of 0.03 m^3 m^{-3} for soil water content measurements in dry soils.

Although multi-offset measurements are widely used in GPR data processing for determining velocity profiles with depth, there are some distinct disadvantages to soil water content determination with this method:

1. As with soil water content determination from single offset measurements, there is no control over the measurement depth resolution.
2. Multi-offset measurements are cumbersome to make and do not allow reconnaissance studies of soil water content variation.
3. For heterogeneous media, soil water content determined from multi-offset measurements is biased toward the common midpoint in the case of a CMP acquisition geometry and toward the position of the fixed antenna in the case of a WARR acquisition geometry (Huisman and Bouten, 2003).

Soil Water Content Measurements with the Ground Wave

The measurement principle of soil water content estimation with the ground wave is illustrated in Fig. 3. The ground wave is the part of the radiated energy that travels between the transmitter and receiver through the top of the soil. The ground wave is detected by the GPR receiver, even in the absence of clearly reflecting soil layers (Du, 1996; Berktold et al., 1998; Sperl, 1999). The evanescent character of the ground wave (see Fig. 2) measured by the GPR receiver antenna at the soil surface requires that both the transmitter and the receiver be placed close to the soil surface.
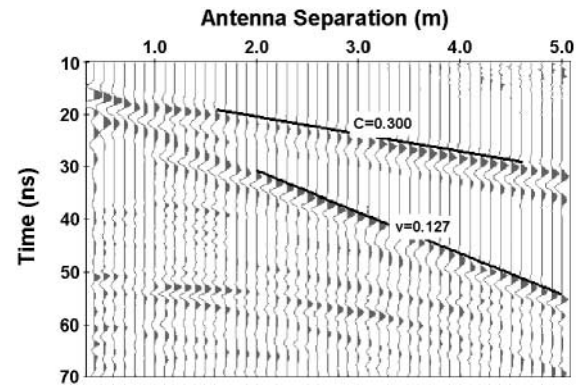
The ground wave can easily be recognized on data collected using a multi-offset GPR acquisition geometry, by the observed linear relationship between antenna separation and ground wave travel times, which starts at the origin of the multi-offset measurement set (see Fig. 6, 7, and 9). The slope of the ground wave in a multi-offset measurement is directly related to the ground wave velocity and can, therefore, be used for soil water content determination. The accuracy of this soil water content measurement technique was determined by Huisman et al. (2001) by analyzing a set of 24 multi-offset measurements collected using 225-MHz antennas and independent gravimetric samples. The resulting calibration equation ($\theta = 0.1087n_a - 0.1076$) is shown in Fig. 10 and has an accuracy of 0.024 m^3 m^{-3}. Grote et al. (2003) compared 29 estimates of water content obtained using multi-offset GPR with independent gravimetric measurements. They reported root mean squared errors of 0.022 and 0.015 m^3 m^{-3} using 450- and 900-MHz antennas, respectively, for calibration equations in the form of Eq. [10]. Both Huisman et al. (2001) and Grote et al. (2003) reported that the permittivity determined from the ground wave velocity also agreed well with the TDR measurements at these frequencies, as is illustrated in Fig. 11 (from Huisman et al., 2001).

Estimation of soil water content using multi-offset GPR measurements is cumbersome and time-consuming, as was mentioned before. The ground wave velocity can also be determined from a single offset GPR measurement, provided that the approximate arrival time of the ground wave is known from a multi-offset GPR measurement. Therefore, Du (1996)
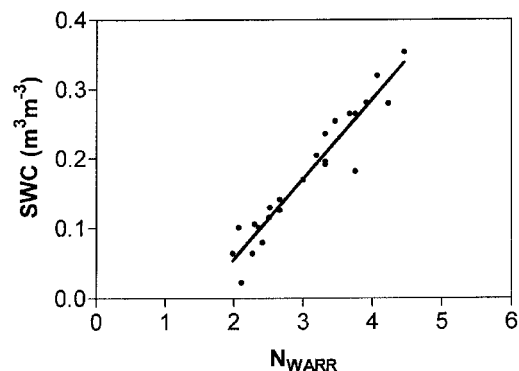
Fig. 10. Calibration equation between gravimetrically determined soil water content (SWC) and refractive index (n_{WARR}) determined from the ground wave velocity obtained with 225-MHz ground penetrating radar (GPR) antennas.
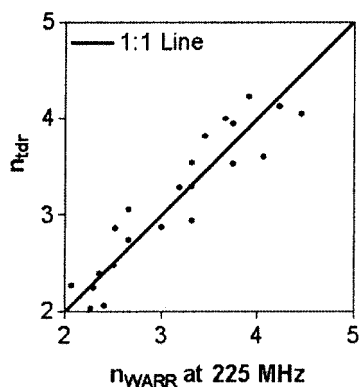
Fig. 11. Comparison of n_{TDR} and n_{WARR} (225 MHz) for the same measurements shown in Fig. 10.

and Sperl (1999) proposed the following procedure for soil water content mapping with the ground wave of GPR:

1. Identify an approximate ground wave arrival time for different antenna separations in a multi-offset GPR measurement,
2. Choose an antenna separation where the ground wave is clearly separated from the air and reflected waves and
3. Use this antenna separation for single offset GPR measurements and relate the changes in ground wave arrival time to changes in soil permittivity.

The most straightforward relationship between ground wave arrival time t_{GW} (s), antenna separation x (m), and soil permittivity is given by Sperl (1999):

$$\varepsilon = \left(\frac{c}{v}\right)^2 = \left[\frac{c(t_{GW} - t_{AW}) + x}{x}\right]^2 \qquad [17]$$

where t_{AW} (s) is the air wave arrival time. The t_{AW} is included as part of the zero time correction, as was already discussed in the previous section. Accurate zero time corrections and accurate travel time determination are important for soil water content measurements derived from ground wave travel time data. Typically, the onset of the wave or the first maximum of the wave are picked, but Huisman and Bouten (2003) showed that these phases can be quite difficult to pick when mapping water content variation, especially for the air wave. Instead, Huisman and Bouten (2003) proposed to use the zero-crossing between the maximum and minimum wave amplitude because the steep derivative of the wave at this phase allows the most accurate travel time determination. It should be noted that the onset of the wave should be preferred over the latter approach when there are clear indications for waveform dispersion (Annan, 1996).

Recent experiments by Lesmes et al. (1999), Hubbard et al. (2002), Huisman et al. (2002, 2003), and Grote et al. (2003) have confirmed that soil water content mapping with ground wave travel time data works well. In an irrigation experiment, Huisman et al. (2002) created a heterogeneous pattern in soil water content by using different types of sprinklers with varying ranges and intensities. Figure 12 (left) shows the increase in water content over a 60 by 60 m area measured with GPR, which was calculated by subtracting the water content map before irrigation from the water content map after irrigation. Ground penetrating radar measurements were made with a 225-MHz antenna on lines 5 m apart. The antenna separation was 1.54 m, and the distance between GPR measurements was 0.5 m. The measurements were performed within 1 h in the field. Time domain reflectometry measurements to 0.1 m deep were made within 1.5 h at 5-m station spacing. The

resulting soil water increase map for TDR is presented in Fig. 12 (right). Clearly, there is a good general agreement between both methods since they show similar patterns in soil water increase caused by the heterogeneous application of water. Furthermore, the higher number of GPR measurements acquired within a shorter time span has resulted in a much higher resolution, as evidenced by the clear circular boundaries of the increase in soil water content due to the impact sprinklers located at (17.5, 42.5) and (35, 25). Using 450- and 900-MHz single offset GPR ground wave data, Grote et al. (2003) estimated the spatial and temporal variations in near surface water content over a large-scale agricultural site during the course of a year. They found that soil texture exerted an influence on the spatial distribution of water content over the field site. Using a 100-MHz antenna, Lesmes et al. (1999) generally found similar trends in soil water content estimated with GPR ground wave data and reference small-scale measurements. However, soil water content estimated using 100-MHz GPR ground wave data typically underestimated water content compared with the reference measurements collected between 0 and 0.30 m below ground surface. This discrepancy may be associated with the deeper zone of influence associated with the lower-frequency GPR antennas as compared with the higher-frequency antennas used in the studies described above.

Although the results with ground wave data generally are promising, there are still some uncertainties associated with this method. An important, but unresolved issue is the effective measurement volume over which the ground wave averages. Du (1996) suggested that the influence depth is approximately one-half of the wavelength [$\lambda = c/(f\varepsilon)^{1/2}$], which would, for example, mean that for a central frequency of 225 MHz, the depth of influence could vary from 0.50 m ($\varepsilon = 4.0$) to 0.22 m ($\varepsilon = 20.0$). Sperl (1999) reported that the depth of influence was indeed a function of wavelength, but from a modeling exercise he concluded that the influence depth is approximately $0.145\lambda^{1/2}$, which would suggest that the influence depth ranges from 0.15 m ($\varepsilon = 4.0$) to 0.10 m ($\varepsilon = 20.0$) for the 225-MHz antennas. The results of Sperl (1999) do not contradict the results of Huisman et al. (2001), who concluded that soil water content measurements based on ground wave data are similar to measurements with 0.10-m-long TDR probes for both the 225- and 450-MHz GPR antennas. Grote et al. (2003) compared estimates of water content obtained using 450- and 900-MHz common offset GPR ground wave data with measurements collected using gravimetric techniques in soils having various textures and at depths from 0 to 0.10, 0.10 to 0.20, and 0 to 0.20 m below ground surface. They found that the estimates obtained using these frequencies showed the highest correlation with the soil water content values averaged across the 0- to 0.20-m range and the least correlation with the water content measurements taken from the 0.10- to 0.20-m interval. Clearly, further research is needed to better understand the ground wave zone of influence.

Other drawbacks of using the GPR ground wave to estimate soil water content include the following:

1. It might be difficult to separate the ground wave arrival in the clutter of critically refracted and reflected waves.
2. It might be difficult to choose an antenna separation for which the arrival times of the air and ground wave can consistently be picked despite moving the antennas across a field with varying soil water content.
3. The ground wave is attenuated more quickly than other waves, which limits the range of antenna separation at which the ground wave can be observed.
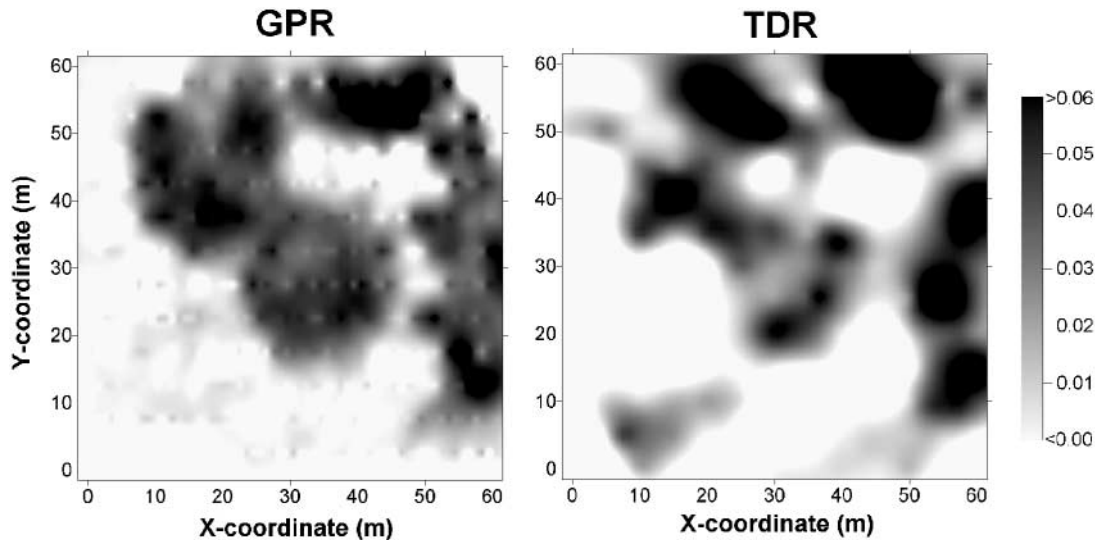
Fig. 12. Maps illustrating the increase in soil water content (m³ m⁻³) due to irrigation obtained using ground penetrating radar (GPR) ground wave and time domain reflectometry (TDR) measurements. The maps were obtained by subtracting interpolated maps of soil water content obtained using GPR and TDR data collected before and after irrigation.

Soil Water Content Measurements with Borehole GPR

For borehole GPR applications, the transmitting and receiving antenna are lowered into a pair of vertical access tubes. In the zero offset profile (ZOP) mode, the antennas are lowered such that their midpoints are always at the same depth (Fig. 13, left). The arrival time of the direct wave between the boreholes and the known borehole separation is used to calculate the velocity and soil permittivity. The ZOP mode is an attractive approach for measuring the soil water content profile of the vadose zone with a high spatial resolution and a large sampling volume (Gilson et al., 1996; Knoll and Clement, 1999; Parkin et al., 2000; Binley et al., 2001, 2002, Rucker and Ferré, 2003). Furthermore, each borehole GPR measurement requires only a couple of seconds and, therefore, the ZOP method is potentially capable of measuring transient processes within the unsaturated zone.

Soil water content can also be determined from a multi-offset profile (MOP, Fig. 13, right). The first arrival times of all multi-offset measurements can be used to reconstruct a (tomographic) two-dimensional image of the soil water content distribution between the boreholes (Hubbard et al., 1997; Parkin et al., 2000; Binley et al., 2001; Alumbaugh et al., 2002). To extract high-resolution, quantitative information from radar tomographic data, it is important to process the data as accurately as possible. The procedure for inverting radar to-

mographic data was presented in detail by Peterson (2001), who also discussed methods for recognizing and correcting for errors caused by incorrect station geometry, incorrect zero time and zero time drift, geometric spreading, transmitter radiation pattern, transmitter amplitude, and high angle raypaths. The two-dimensional tomogram is obtained by discretizing the area between the boreholes in rectangular cells of constant velocity and determining the velocity of each cell by minimizing the difference between measured arrival times and arrival times calculated for raypaths passing through these cells. When necessary, three-dimensional tomograms can also be reconstructed (e.g., Eppstein and Dougherty, 1998). The drawback of acquiring the two-dimensional tomogram is the much longer time (typically several hours) required to obtain all the required measurements. Therefore, the MOP mode is best suited for steady-state water content conditions. For cases where the subsurface variations occur on similar time scales as the radar data acquisition, Day-Lewis et al. (2002) recently described a sequential approach for inverting time-lapse tomographic radar data to assist in more accurate imaging.

The sampling volume of borehole GPR measurements can be approximated by the volume of the first Fresnel zone (Cerveny and Soares, 1992). The Fresnel volume is an elongated rotational ellipsoid with its foci at the location of the transmitter and the receiver. For a homogeneous medium, the Fresnel volume, V, depends on the path length of the ray trace, L (m), and the wavelength of the radar signal, λ (m):

$$V = \frac{4}{3}\pi abc \qquad [18]$$

where a, b, and c are the semi-axes of the ellipsoid defined as

$$a = \frac{1}{2}\left(\frac{\lambda}{2} + L\right) \qquad [19]$$

$$b,c = \frac{1}{2}\left(\frac{\lambda^2}{4} + L\lambda\right)^{\frac{1}{2}} \qquad [20]$$

The wavelength, λ, can be calculated from the center frequency or the bandwidth of the transmitted GPR pulse. The Fresnel zone, a circular region, is the cross section of the Fresnel volume in a plane perpendicular to the raypath. The maxi-
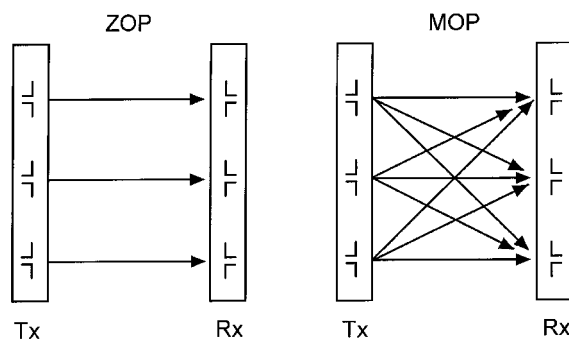
Fig. 13. Schematic diagrams of borehole ground penetrating radar (GPR) wave paths between transmitter and receiver for ZOP (left) and MOP (right).

mum diameter of the Fresnel zone along the raypath (2*b*) is often given as the spatial resolution in tomography.

Several studies have compared water content estimates obtained from GPR travel time data collected between boreholes with one-dimensional measurements obtained from data collected within the corresponding boreholes (Hubbard et al., 1997; Binley et al., 2001; Alumbaugh et al., 2002). Errors in water content estimates obtained using borehole GPR data can potentially arise from acquisition procedures (ZOP and MOP), inversion procedures (MOP), as well as from the petrophysical relationship used to convert the GPR velocity estimates to water content (ZOP and MOP). Using a site-specific petrophysical relationship, Alumbaugh et al. (2002) found that estimates of volumetric water content obtained from tomographic radar velocity estimates had a root mean square error of 0.02 to 0.03 m^3 m^{-3} compared with neutron log derived values obtained from corresponding boreholes, and that the errors were greatest in wetter zones. Repeatability measurements at the same study site suggested that the precision associated with the radar acquisition system accounted for about 0.5% of the error in water content estimation.

Time-lapse radar tomograms are often presented as "difference" tomograms to illustrate the change in geophysical attribute (or corresponding estimated moisture content) with time. These tomograms are constructed by subtracting the geophysical responses collected at one point in time from the responses collected at the same location but at another point in time, or by inverting the differences in the electromagnetic travel time picks. By displaying differences only, subtle changes associated with a dynamic event, such as moisture migration due to forced or natural infiltration, can be highlighted. For example, if the geophysical signal is influenced by both lithology and moisture content in the unsaturated zone, by collecting data during an infiltration experiment at one point in time and subtracting it from another data set collected at another point in time, the changes in the geophysical signature associated only with the infiltrating fluid are illuminated, and the effects of the geology are suppressed. This approach has been used with time-lapse radar tomographic data to delineate permeable pathways and moisture migration (Hubbard et al., 1997; Eppstein and Dougherty, 1998). Binley et al. (2002) converted time lapse ZOP radar data sets to volumetric water content using a dielectric mixing model (West et al., 2003) to obtain an estimated change in volumetric water content. Their change in water content estimates ranged between 0.5 and 2% and agreed favorably with monthly rainfall measurements.

As described by Peterson (2001), extreme care must be taken to determine the zero time when using crosshole radar data for time-lapse monitoring, as zero time drift associated with the radar system can easily overwhelm velocity changes caused by the dynamic event that is being monitored. These changes can be caused by system electronics, such as changing power transmitters or cycling the power to any of the system components. Loose connections or temperature changes as the system components warm up can cause more subtle shifts. Peterson (2001) suggested collecting ZOP data prior and subsequent to acquiring MOP radar data to assess zero time drifts that occur during acquisition and subsequently accounting for them in the MOP processing procedure.

A comparison between estimates of water content obtained from simple transformations of data obtained using 200-MHz borehole GPR and logging tools is given in Fig. 14 (modified from Majer et al., 2002). These data were collected within a sandy and unsaturated section of the DOE Hanford Site in Washington. Figure 14a illustrates estimates of soil water content (SWC) obtained at two well bores (X2 and X3) using cone penetrometer (CPT) capacitance probe measurements (Shinn

et al., 1998). In Fig. 14b, the solid lines illustrate the soil water content estimates obtained from the ZOP measurements, acquired prior and subsequent to the MOP measurements, while the dashed line indicates the estimates obtained from the ZOP measurements extracted from the MOP gathers. These ZOP measurements have been converted into water content using the Topp relation and without accounting for the zero time drift as was mentioned above and described in detail by Peterson (2001). A gradual shift in zero time is illustrated by this figure, which is indicative of system changes associated with components in the radar system warming up. This figure highlights how important it is to correct for zero time drifts using radar tomographic data. For example, in this case, if the zero time drift is not accounted for, estimates of soil water content obtained from radar velocity measurements could easily be off by 1%. Finally, Fig. 14c illustrates the estimates of soil water content obtained by converting the tomographic (MOP) travel time data, collected between X2 and X3 and corrected for zero time drift, into estimates of water content using the Topp relation. Comparison of the estimates of water content from the one-dimensional CPT data, the horizontally averaged ZOP data, and the two-dimensional tomographic data illustrate the similarity in water content spatial distributions revealed by the borehole GPR estimates and the log data under conditions of only minor lateral heterogeneity. Similar results have been found on comparison of water content estimates obtained from borehole GPR and from neutron probe data.

Crucial to the analysis of borehole GPR measurements is the correct identification of the raypath of the wave arriving first (Hammon et al., 2003; Rucker and Ferré, 2003; Ferré et al., 2003). Figure 15 (left) shows possible raypaths for ZOP measurements in a soil with a high-velocity (dry) layer surrounded by soil with a lower velocity. Figure 15 (right) presents the corresponding schematic ZOP measurement (right). For the high-velocity zone, the direct wave labeled 1 arrives first, and the known borehole separation can be used to calculate the velocity. The reflections from the top and bottom of the high velocity zone (marked 2 and 3) arrive later. When the antennas are in the low-velocity zone, refracted waves (4 and 5), rather than direct waves (6), might arrive first, and the velocity estimate will be in error when a direct wave path is assumed. This is of particular importance for borehole GPR measurements near the surface, where the refracted (air) wave (4) will most likely arrive first. For refracted waves partly traveling in air, the velocity–depth profile, $V(z)$ can be estimated from (Hammon et al., 2003)

$$V(z) = \frac{1}{\sqrt{\frac{1}{c^2} + \frac{1}{4V'(z)^2}}} \qquad [21]$$

where $V'(z)$ is the apparent velocity at depth z that can be determined from the slope, dz/dt, in Fig. 14 (right). Rucker and Ferré (2003) successfully used Eq. [21] to determine soil water content from refracted air waves. They also predicted refraction termination depths below which direct waves are expected to arrive before refracted air waves, which can be helpful in analyzing borehole GPR measurements.

Borehole GPR has not only been used in the vertical ZOP and MOP mode. For example, Parkin et al. (2000) and Galagedara et al. (2002) used horizontal boreholes to monitor the soil water content in a two-dimensional horizontal plane below a wastewater trench. Other interesting applications of horizontal boreholes are conceivable, such as measurements of fingered flow and solute breakthrough. Knoll and Clement (1999) and Buursink et al. (2002) used an acquisition scheme
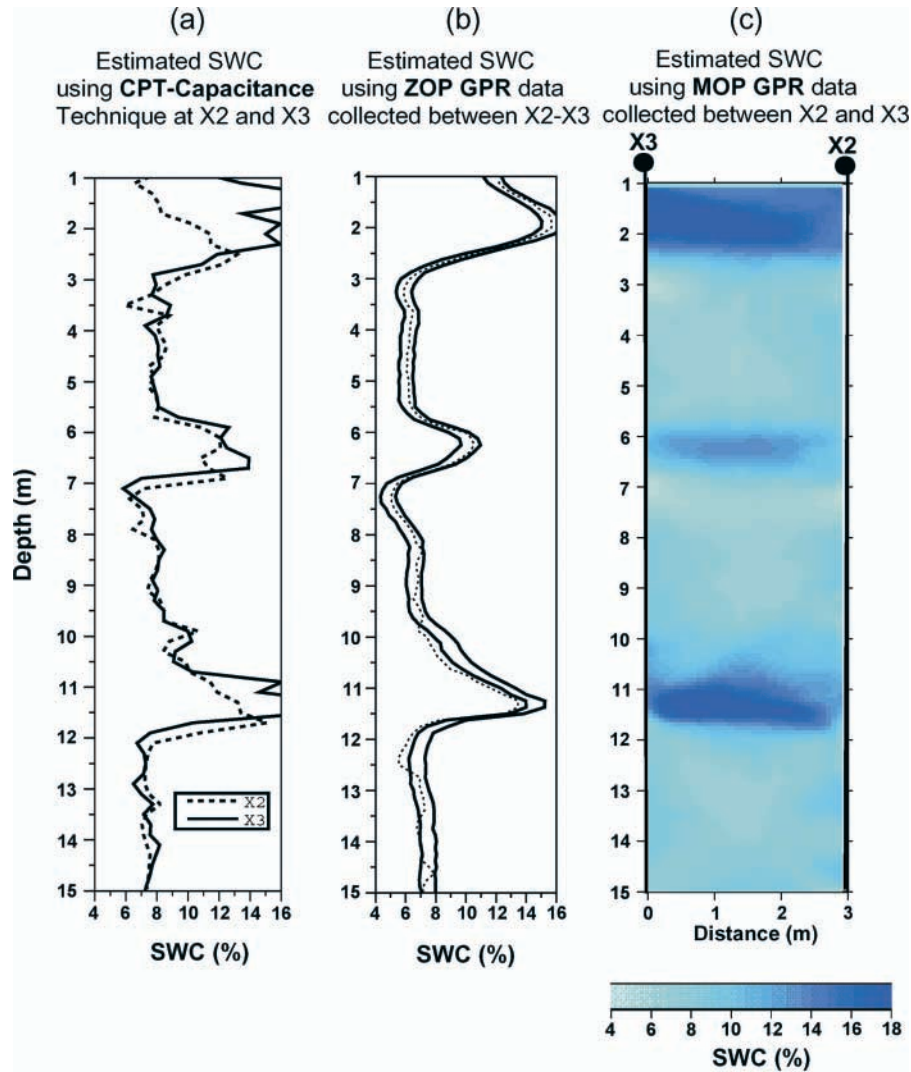
Fig. 14. A comparison between estimates of soil water content (SWC) obtained from simple transformations of 200-MHz zero offset profiling (ZOP) and multi-offset profiling (MOP) borehole ground penetrating radar (GPR) as well as cone penetrometer (CPT) data at the DOE Hanford Site in Washington (modified from Majer et al., 2002).

called vertical radar profiling (VRP) to estimate water content. In VRP, one antenna is moved down the borehole while the other antenna remains stationary at the soil surface. As with conventional borehole acquisition schemes, the travel time of the direct arrivals is determined to estimate water content. The advantage of VRP over the other borehole GPR acquisition

schemes is that only one borehole is required. However, the use of only one borehole restricts the depth of investigation and reduces the accuracy as compared with the ZOP and MOP acquisition schemes.

An interesting extension of borehole GPR inversion procedures is the consideration of radar velocity anisotropy (Vasco
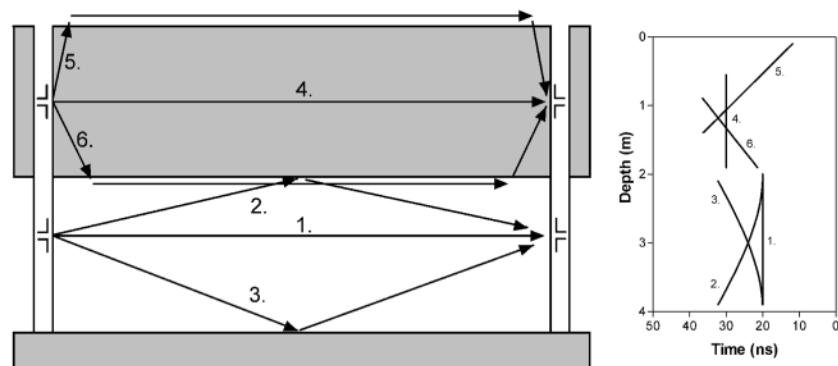
Fig. 15. Schematic raypaths (left) and common-offset data (right) for borehole ground penetrating radar (GPR) measurements made in a soil with a high velocity layer.

Fig. 16. An elevated 500-MHz ground penetrating radar (GPR) system being used to measure surface reflection amplitude.

Fig. 17. Water content profiles measured with air-launched 500-MHz ground penetrating radar (GPR) surface reflectivity method compared with measurements obtained using 20-cm-long time domain reflectometry (TDR) probes.

et al., 1997) and the simultaneous analysis of velocity and attenuation (e.g., Ollson et al., 1992; Zhou et al., 2001). Considering the impact of simultaneous measurement of bulk permittivity and bulk soil conductivity with TDR in soil physics and hydrology (e.g., Robinson et al., 2003), it seems worthwhile to direct more attention to this type of borehole GPR application.

Recent publications show that borehole GPR is quickly becoming an important site-specific investigation tool in hydrogeological studies. An obvious but important difference from the other GPR methods presented in this review is that borehole GPR is not suitable as a reconnaissance tool. Despite the strong increase of borehole GPR applications, there are several points that require attention when using this technique:

1. To obtain quantitative information from borehole radar data, it is important to recognize and correct for errors caused by acquisition procedures and transmission characteristics as described by Peterson (2001), and to recognize the accuracy limitations as described by Alumbaugh et al. (2002).
2. It is important to consider the impact of refracted waves, especially those traveling in the soil (labeled 6 in Fig. 14), on the accuracy of soil water content measurements with borehole GPR.
3. The length of the borehole GPR antenna, the borehole separation distance, and the antenna frequencies have an impact on the maximum spatial resolution that can be achieved;
4. Soil heterogeneity affects the sampling volume of borehole GPR.

Soil Water Content Measurements with Surface Reflections

The measurement principle of soil water content measurements with air-launched surface reflections is illustrated in Fig. 16. The GPR antennas are operated at some distance above the ground by mounting them on a vehicle or a low-flying air platform. The soil property being measured is the reflection coefficient of the air–soil interface, R, which is related to the soil permittivity, ε_{soil}, by

$$R = \frac{1 - \sqrt{\varepsilon_{soil}}}{1 + \sqrt{\varepsilon_{soil}}} \qquad [22]$$

The reflection coefficient is determined from the measured amplitude, A_r, relative to the amplitude of a "perfect" reflector, A_m, such as a metal plate larger than the footprint of the
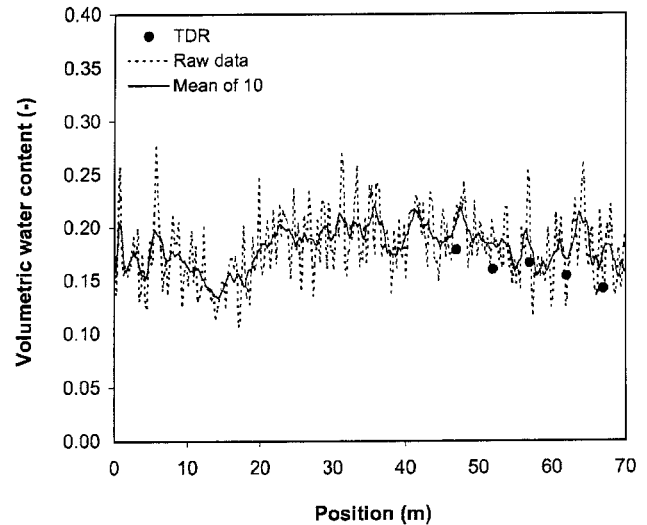
radar (Davis and Annan, 2002; Redman et al., 2002):

$$\varepsilon_{soil} = \left(\frac{1 + \dfrac{A_r}{A_m}}{1 - \dfrac{A_r}{A_m}} \right)^2 \qquad [23]$$

The ε_{soil} obtained from surface reflectivity is a nonlinear average of the permittivity variation with depth. The footprint of the radar can be approximated by the diameter of the first Fresnel zone (FZD):

$$FZD = \left(\frac{\lambda^2}{4} + 2h\lambda \right)^{0.5} \qquad [24]$$

where λ is the wavelength (c/f for air) at the center frequency of the GPR antenna and h is the height of the antenna above the surface. Although the definition of the FZD applies to a monochromatic source, it has been shown that this is also a good approximation for surface reflectivity measurements performed with GPR, which uses a broadband source (Redman et al., 2002). The FZD criterion suggests a calibration footprint of 0.79 by 0.79 m for 1-GHz antennas operated 1.0 m above the soil surface and a footprint of 1.76 by 1.76 m for 225-MHz antennas operated at the same height. Clearly, surface reflection measurements are more practical with high-frequency GPR antennas.

Figure 17 shows a sample of data acquired with the 500-MHz GPR surface reflection measurement set up shown in Fig. 16. Generally, the soil water content measured with GPR is similar to the soil water content measured with 0.20-m-long TDR sensors. However, there seems to be quite a large amount of very short distance variation in soil water content, which was also reported by Redman et al. (2002). Three likely explanations for the observed large variation of ± 0.10 m^3 m^{-3} in soil water content include (i) the impact of the soil water content profile with depth on the reflection coefficient, (ii) the impact of surface roughness on the reflection coefficient, and (iii) reliability and accuracy of amplitude measurements.

The determination of soil water content from the reflection coefficient requires accurate amplitude measurements. Figure
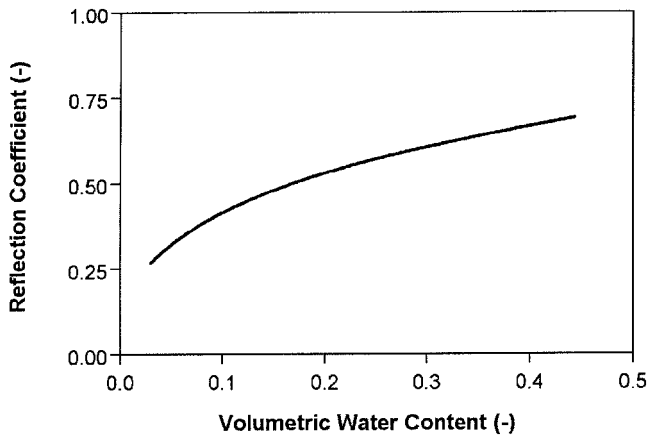
Fig. 18. Reflection coefficient as a function of soil water content. Soil water content was calculated from soil permittivity with Topp's equation (Eq. [6]).

18 shows the relation between the reflection coefficient associated with the air–soil interface and soil water content, assuming Topp's equation for the relation between soil permittivity and soil water content. The relationship reveals that the reflection coefficients are more sensitive to variations in SWC at lower water content ranges than at higher water content ranges. Simple calculations show that an error of only 1% in measured amplitudes can result in a significant error of ± 0.02 m^3 m^{-3} for a soil water content of 0.30 m^3 m^{-3}. Redman et al. (2002) reported that measured repeat profiles have typical differences of <0.02 m^3 m^{-3}, which suggests that the required accurate amplitude measurements can be achieved with the current generation of GPR instrumentation and that the amplitude accuracy was not a major contributor to the observed variability in Fig. 17.

Surface roughness and varying soil water content profiles with depth will both cause significant scattering, which leads to a decrease in reflection coefficient and an underestimation of soil water content if it is not accounted for. Chanzy et al. (1996) used the Rayleigh criterion (~1/8 of the wavelength) to determine the upper limit of surface roughness, below which the surface can be considered smooth. For example, for the 1-GHz antennas the surface roughness must be below 0.038 m for an adequate approximation of a smooth surface, and for the 225-MHz a surface roughness below 0.167 m is sufficient. The Rayleigh criterion implies that lower antenna frequencies will be less sensitive to surface roughness and will, therefore, show less soil water content variation, which was confirmed by Redman et al. (2002). The effective measurement depth and the impact of soil water content variations with depth are topics of active research, but little is known at the moment.

Clearly, the impact of surface roughness and soil water content profiles on the surface reflection coefficient are two key issues that need to be addressed when applying this technique. It is interesting to note that these problems are similar to those in active remote sensing (e.g., Jackson et al., 1996), and it is possible that this soil water content measurement technique can profit from developments in the highly sponsored field of remote sensing.

GROUND PENETRATING RADAR INSTRUMENTATION

There are a number of commercial GPR systems available on the market. The three largest manufacturers are Geophysical Survey Systems Incorporated (GSSI, North Salem, NH;

www.geophysical.com), Malå Geosciences (Malå, Sweden; www.malags.se), and Sensors and Software (Mississauga, ON, Canada; www.sensoft.ca). These manufacturers provide multipurpose GPR systems that can typically be operated at different frequency ranges from 10 to 1400 MHz. The GPR market as a whole is moving toward easy-to-use GPR systems dedicated to specific tasks. Besides the aforementioned manufacturers of GPR equipment, there are other manufacturers, who mostly provide purpose-built systems operating at around 1000 MHz (Davis and Annan, 2002).

Important aspects to note when choosing a GPR system for soil water content measurements include the availability of the required range of antenna frequencies, the possibility to separate antennas for multi-offset measurements, and the availability of borehole antennas. It is also useful to have shielded antennas for higher quality measurements in the presence of cultural noise. Some GPR systems allow multichannel acquisition, which can considerably speed up the acquisition of multi-offset data. Although this is helpful for soil water content measurements based on reflected wave and ground wave data, it remains to been seen whether the extra costs of multiple antennas is worth the reduced acquisition effort for hydrological applications.

In many studies, accurate positioning of radar measurements is important. Traditional surveying with marked positions in the field is very time-consuming. Most GPR systems allow interfacing with a GPS, which can provide the freedom of movement not available in traditional surveying. However, for some applications the accuracy of regular GPS systems might not be sufficient. Higher positional accuracy can be obtained by more advanced differential GPS systems or by a self-tracking theodolite (e.g., Lehmann and Green, 1999).

CONCLUSION

In this review, we have presented an overview of the available methods for measuring soil water content with GPR. Although the GPR technology has been developed in the same period as the successful TDR methodology, there is still a large difference in acceptance between these methods for soil water content determination. This can partly be attributed to the limited suitability of the first generation GPR instrumentation for accurate soil water content measurements. However, the current generation of GPR instrumentation provides much more accurate measurements, which has resulted in a revival of the use of GPR for water content determination as evidenced by the increasing number of publications in recent years.

The extensive research in the past years on all of the available methods has clearly demonstrated that GPR can be used by experienced researchers to provide reliable estimates of subsurface water content. The exception to this is the GPR surface reflectivity method that, although promising, does not yet provide the accuracy and robustness of the other methods. In our opinion, the complexity of data acquisition and processing currently limits the applicability of GPR for water content estimation to the research community. However, continued development of specific and easy-to-use GPR instrumentation, coupled with increased experience and application of GPR for water content estimation, should help to bridge the gap between the advances made in the research community and the practical need for straight-

forward tools to accurately measure water content in high resolution and over large areas. Most likely, the borehole GPR method will continue to be used as an important research tool for studying infiltration processes and contaminant transport in the saturated and unsaturated zones. There may even be potential applications outside the research community for monitoring subsurface water content as part of groundwater protection strategies.

The potential and limitations of each GPR method for water content determination have been discussed extensively in this review. Here, we want to highlight two important research issues that, in our opinion, currently limit the development and acceptance of GPR as a soil water content sensor. The first issue deals with the petrophysical relationships between permittivity and volumetric water content. Although the community seems to have high confidence in the reliability of these relationships because of the excellent results obtained with TDR, there seems to be evidence that site- and frequency-dependent relationships may be required for those applications that require accurate water content measurements with lower-frequency GPR antennas. Further measurements of the frequency dependency of soil permittivity in the 10-MHz to 1-GHz frequency range and further field studies that directly compare TDR and GPR using lower-frequency antennas on high clay content soils should help resolve this issue. The second issue is the sampling volume and spatial resolution of all of the GPR methods, particularly under heterogeneous (field) conditions. Here, both numerical modeling and field studies will be required to determine these values.

ACKNOWLEDGMENTS

REFERENCES

Alumbaugh, D., P. Chang, L. Paprocki, J. Brainard, R.J. Glass, and C.A. Rautman. 2002. Estimating moisture contents in the vadose zone using cross-borehole ground penetrating radar: A study of accuracy and repeatability. Water Resour. Res. 38:1309.

Annan, A.P. 1973. Radar interferometry depth sounding: Part I. Theoretical discussion. Geophysics 38:557–580.

Annan, A.P. 1996. Transmission, dispersion and GPR. J. Environ. Eng. Geophys. 0:125–136.

Berktold, A., K.G. Wollny, and H. Alstetter. 1998. Subsurface moisture determination with the ground wave of GPR. p. 675–680. *In* Proc. Int. Conf. on Ground-Penetrating Radar, 7th, Lawrence, KS. May 1998. Univ. of Kansas, Lawrence.

Binley, A., P. Winship, R. Middleton, M. Pokar, and J. West. 2001. High-resolution characterization of vadose zone dynamics using cross-borehole radar. Water Resour. Res. 37:2639–2652.

Binley, A., P. Winship, L.J. West, M. Pokar, and R. Middleton. 2002. Seasonal variation of moisture content in unsaturated sandstone inferred from borehole radar and resistivity profiles. J. Hydrol. (Amsterdam) 267:160–172.

Bohidar, R.N., and J.F. Hermance. 2002. The GPR refraction method. Geophysics 67:1474–1485.

Buursink, M.L., J.W. Lane, Jr., W.P. Clement, and M.D. Knoll. 2002. Use of vertical-radar profiling to estimate porosity at two New England sites and comparison with neutron log porosity. *In* Proc. of SAGEEP '02, Las Vegas, NV. 10–14 Feb. 2002. Environmental and Engineering Geophysical Society, Denver, CO.

Callies, U., A. Rhodin, and D.P. Eppel. 1998. A case study on variational soil moisture analysis from atmospheric observations. J. Hydrol. (Amsterdam) 212–213:95–108.

Cerveny, V., and J.E.P. Soares. 1992. Fresnel volume ray tracing. Geophysics 57:902–915.

Chanzy, A., A. Tarussov, A. Judge, and F. Bonn. 1996. Soil water content determination using a digital ground-penetrating radar. Soil Sci. Soc. Am. J. 60:1318–1326.

Dalton, F.N., W.N. Herkelrath, D.S. Rawlins, and J.D. Rhoades. 1984. Time-domain reflectometry: Simultaneous measurement of soil water content and electrical conductivity with a single probe. Science 224:989–990.

Dannowski, G., and U. Yaramanci. 1999. Estimation of water content and porosity using combined radar and geoelectrical measurements. Eur. J. Environ. Eng. Geophys. 4:71–85.

Davis, J.L., and A.P. Annan. 1989. Ground-penetrating radar for high resolution mapping of soil and rock stratigraphy. Geophys. Prospect. 37:531–551.

Davis, J.L., and A.P. Annan. 2002. Ground penetrating radar to measure soil water content. p. 446–463. *In* J.H. Dane and G.C. Topp (ed.) Methods of soil analysis. Part 4. SSSA Book Ser. 5. SSSA, Madison WI.

Day-Lewis, F.D., J.M. Harris, and S. Gorelick. 2002. Time-lapse inversion of crosswell radar data. Geophysics 67:1740–1752.

Debye, P. 1929. Polar molecules. Dover Publ., Mineola, NY.

Dix, C.H. 1955. Seismic velocities from surface measurements. Geophysics 20:73.

Dobson, M.C., F.T. Ulaby, M.T. Hallikainen, and M.A. El-Rayes. 1985. Microwave dielectric behaviour of wet soil. Part II. Dielectric mixing models. IEEE Trans. Geosci. Remote Sens. 23:35–46.

Du, S. 1996. Determination of water content in the subsurface with the ground wave of ground penetrating radar. Ph.D. thesis. Ludwig-Maximilians-Universität, Munich, Germany.

Endres, A.L., W.P. Clement, and D.L. Rudolph. 2000. Ground penetrating radar imaging of an aquifer during a pumping test. Ground Water 38:566–576.

Entekhabi, D., G.R. Asrar, A.K. Betts, K.J. Beven, R.L. Bras, C.J. Duffy, T. Dunne, R.D. Koster, D.P. Lettenmaier, D.B. McLaughlin, W.J. Shuttleworth, M.Th. van Genuchten, M.Y. Wei, and E.F. Wood. 1999. An agenda for land surface hydrology research and a call for the second international hydrological decade. Bull. Am. Meteorol. Soc. 80:2043–2058.

Eppstein, M.J., and D.E. Dougherty. 1998. Efficient three-dimensional data inversion: Soil characterization and moisture monitoring from cross-well ground-penetrating radar at a Vermont test site. Wat. Resour. Res. 34:1889–1900.

Famiglietti, J.S., J.A. Deveraux, C.A. Laymon, T. Tsegaye, P.R. Houser, T.J. Jackson, S.T. Graham, M. Rodell, and P.J. van Oevelen. 1999. Ground-based investigation of soil moisture variability within remote sensing footprints during the Southern Great Plains 1997 (SGP97) hydrology experiment. Wat. Resour. Res. 35: 1839–1851.

Ferré, P.A., D.L. Rudolph, and R.G. Kachanoski. 1996. Spatial averaging of water content by time domain reflectometry: Implications for twin rod probes with and without dielectric coatings. Wat. Resour. Res. 32:271–279.

Ferré, P.A., G. von Glinski, and L.A. Ferré. 2003. Monitoring the maximum depth of drainage in response to pumping using borehole ground penetrating radar. Available at www.vadosezonejournal. org. Vadose Zone J. 2:511–518 (this issue).

Friedman, S.P. 1998. A saturation degree-dependent composite spheres model for describing the effective dielectric constant of unsaturated porous media. Wat. Resour. Res. 34:2949–2961.

Galagedara, L.W., G.W. Parkin, J.D. Redman, and A.L. Endres. 2002. Temporal and spatial variation of soil water content measured by borehole GPR under irrigation and drainage. Proc. of the Ninth Conf. on Ground Penetrating Radar. Proc. SPIE 4758:180–185.

Garambois, S., P. Senechal, and H. Perroud. 2002. On the use of combined geophysical methods to assess water content and water conductivity of near-surface formations. J. Hydrol. (Amsterdam) 259:32–48.

Gilson, E.W., J.D. Redman, J. Pilon, and A.P. Annan. 1996. Near surface applications of borehole radar. p. 545–553. *In* Proc. of the Symp. on the Application of Geophysics to Engineering and Environmental Problems, Keystone, CO. Environ. Eng. and Geophys. Soc., Denver, CO.

Greaves, R.J., D.P. Lesmes, J.M. Lee, and M.N. Toksoz. 1996. Velocity variations and water content estimated from multi-offset, ground-penetrating radar. Geophysics 61:683–695.

Grote, K., S.S. Hubbard, and Y. Rubin. 2002. GPR monitoring of volumetric water content in soils applied to highway construction and maintenance. Leading Edge Explor. 21:482–485.

Grote, K., S.S. Hubbard, and Y. Rubin. 2003. Field-scale estimation of volumetric water content using GPR ground wave techniques. Wat. Resour. Res. In press.

Hammon, W.S. III, X. Zeng, R.M. Corbeanu, and G.A. McMechan. 2003. Estimation of the spatial distribution of fluid permeability from surface and tomographic GPR data and core, with a 2-D example from the Ferron Sandstone, Utah. Geophysics 67:1505–1515.

Hasted, J.B. 1973. Aqueous dielectrics. Chapman and Hall, London.

Heimovaara, T.J., and W. Bouten. 1990. A computer-controlled 36-channel time domain reflectometry system for monitoring soil water contents. Water Resour. Res. 26:2311–2316.

Herkelrath, W.N., S.P. Hamburg, and F. Murphy. 1991. Automatic, real-time monitoring of soil moisture in a remote field area with time domain reflectometry. Water Resour. Res. 27:857–864.

Hubbard, S.S., K. Grote, and Y. Rubin. 2002. Mapping the volumetric soil water content of a California vineyard using high-frequency GPR ground wave data. Leading Edge Explor. 21:552–559.

Hubbard, S.S., J.E. Peterson, Jr., E.L. Majer, P.T. Zawislanski, K.H. Williams, J. Roberts, and F. Wobber. 1997. Estimation of permeable pathways and water content using tomographic radar data. Leading Edge Explor. 16:1623–1630.

Huisman, J.A., and W. Bouten. 2003. Accuracy and reproducibility of measuring soil water content with the ground wave of ground penetrating radar. J. Environ. Eng. Geophys. 8:65–73.

Huisman, J.A., J.J.J.C. Snepvangers, W. Bouten, and G.B.M. Heuvelink. 2002. Mapping spatial variation in surface soil water content: Comparison of ground-penetrating radar and time domain reflectometry. J. Hydrol. (Amsterdam) 269:194–207.

Huisman, J.A., J.J.J.C. Snepvangers, W. Bouten, and G.B.M. Heuvelink. 2003. Monitoring temporal development of spatial soil water content variation: Comparison of ground penetrating radar and time domain reflectometry. Available at www.vadosezonejournal.org. Vadose Zone J. 2:519–529 (this issue).

Huisman, J.A., C. Sperl, W. Bouten, and J.M. Verstraten. 2001. Soil water content measurements at different scales: Accuracy of time domain reflectometry and ground-penetrating radar. J. Hydrol. (Amsterdam) 245:48–58.

Jackson, T.J., J. Schmugge, and E.T. Engman. 1996. Remote sensing applications to hydrology: Soil moisture. Hydrol. Sci. J. 41:517–530.

Jacobsen, O.H., and P. Schjønning. 1994. Comparison of TDR calibration functions for soil water determination. p. 9–23. *In* Proc. Time Domain Reflectometry, Applications in Soil Science, Research Centre Foulum, Denmark. 16 Sept. 1994. SP-Report 25-33. Danish Inst. of Plant and Soil Sci., Tjele, Denmark.

Jones, S.B., and S.P. Friedman. 2000. Particle shape effect on the effective permittivity of anisotropic or isotropic media consisting of aligned or randomly oriented ellipsoidal particles. Water Resour. Res. 36:2821–2833.

Knoll, M.D., and W.P. Clement. 1999. Vertical radar profiling to determine dielectric constant, water content and porosity values at well locations. p. 821–830. *In* Proc. of SAGEEP'99, Oakland, CA. Environ. Eng. and Geophys. Soc., Denver, CO.

Ledieu, J., P. De Ridder, P. De Clerck, and S. Dautrebande. 1986. A method of measuring soil moisture by time domain reflectometry. J. Hydrol. (Amsterdam) 88:319–328.

Lehmann, F., and A.G. Green. 1999. Semi-automated georadar data acquisition in three dimensions. Geophysics 64:719–731.

Lesmes, D.P., R. Herbstzuber, and D. Wertz. 1999. Terrain permittivity mapping: GPR measurements of near-surface soil moisture. p. 575–582. *In* Proc. SAGEEP'99, Oakland, CA. Environ. Eng. and Geophys. Soc., Denver, CO.

Majer, E.L., K.H. Williams, J.E. Peterson, and T.M. Daley. 2002. High resolution imaging of vadose zone transport using crosswell radar and seismic methods. Rep. LBNL 49022. Lawrence Berkeley National Laboratory, Berkeley, Ca.

Merz, B., and A. Bardossy. 1998. Effects of spatial variability on the rainfall runoff process in a small loess catchment. J. Hydrol. (Amsterdam) 212–213:304–317.

Merz, B., and E.J. Plate. 1997. An analysis of the effects of spatial variability of soil and soil moisture on runoff. Water Resour. Res. 33:2909–2922.

Nakashima, Y., H. Zhou, and M. Sato. 2001. Estimation of groundwater level by GPR in an area with multiple ambiguous reflections. J. Appl. Geophys. 47:241–249.

Nelson, S.O. 1994. Measurement of microwave dielectric properties of particulate materials. J. Food Eng. 21:365–384.

Olhoeft, G.R. 1987. Electrical properties from 10^{-3} to 10^{+9} Hz: Physics and chemistry. Proc. Phys. Chem. Porous Media II 154:281–298.

Ollson, O., L. Falk, O. Forslund, L. Lundmark, and E. Sandberg. 1992. Borehole radar applied to the characterization of hydraulically conductive fracture zones in crystalline rock. Geophys. Prospect. 40:109–142.

Or, D., and J.M. Wraith. 1999. Temperature effects on soil bulk dielectric permittivity measured by time domain reflectometry: A physical model. Water Resour. Res. 35:371–383.

Parkin, G., D. Redman, P. von Bertoldi, and Z. Zhang. 2000. Measurement of soil water content below a wastewater trench using ground-penetrating radar. Water Resour. Res. 36:2147–2154.

Pauwels, V.R.N., R. Hoeben, N.E.C. Verhoest, and F.P. De Troch. 2001. The importance of the spatial patterns of remotely sensed soil moisture in the improvement of discharge predictions for small-scale basins through data assimilation. J. Hydrol. (Amsterdam) 251:88–102.

Peterson, J.E., Jr. 2001. Pre-inversion corrections and analysis of radar tomographic data. J. Environ. Eng. Geophys. 6:1–18.

Redman, J.D., J.L. Davis, L.W. Galagedara, and G.W. Parkin. 2002. Field studies of GPR air launched surface reflectivity measurements of soil water content. Proc. of the Ninth Conf. on Ground-Penetrating Radar. Proc. SPIE 4758:156–161.

Robinson, D.A., S.B. Jones, J.M. Wraith, D. Or, and S.P. Friedman. 2003. A review of advances in dielelectric and electric conductivity measurements using time domain reflectometry. Available at www.vadosezonejournal. Vadose Zone J. 2:444–475 (this issue).

Roth, K., R. Schulin, H. Flühler, and W. Attinger. 1990. Calibration of time domain reflectometry for water content measurement using a composite dielectric approach. Water Resour. Res. 26:2267–2273.

Rubin, Y. 2003. Applied stochastic hydrogeology. Oxford University Press, Oxford, UK.

Rucker, D.F., and P.A. Ferré. 2003. Near-surface water content estimation with borehole ground penetrating radar using critically refracted waves. Available at www.vadosezonejournal.org. Vadose Zone J. 2:247–252.

Shinn, J.D., D.A. Timian, R.M. Morey, G. Mitchell, C.L. Antle, and R. Hull. 1998. Development of a CPT deployed probe for in situ measurement of volumetric soil moisture content and electrical resistivity. Field Anal. Chem. Tech. 2:103–109.

Sperl, C. 1999. Determination of spatial and temporal variation of the soil water content in an agro-ecosystem with ground-penetrating radar. (In German.) Ph.D. thesis. Technische Universitat München, Munich, Germany.

Stoffregen, H., T. Zenker, and G. Wessolek. 2002. Accuracy of soil water content measurements using ground penetrating radar: Comparison of ground penetrating radar and lysimeter data. J. Hydrol. (Amsterdam) 267:201–206.

Tillard, S., and J.-C. Dubois. 1995. Analysis of GPR data: Wave propagation velocity determination. J. Appl. Geophys. 33:77–91.

Topp, G.C., J.L. Davis, and A.P. Annan. 1980. Electromagnetic determination of soil water content: Measurements in coaxial transmission lines. Water Resour. Res. 16:574–582.

Topp, G.C., M. Yanuka, W.D. Zebchuk, and S.J. Zegelin. 1988. Determination of electrical conductivity using time domain reflectometry: Soil and water experiments in coaxial lines. Water Resour. Res. 24:945–952.

Ulaby, F.T., P.C. Dubois, and J. van Zyl. 1996. Radar mapping of surface soil moisture. J. Hydrol. (Amsterdam) 184:57–84.

van Dam, R.L., W. Schlager, M.J. Dekkers, and J.A. Huisman. 2002. Iron oxides as a cause of GPR reflections. Geophysics 67:536–545.

van Oevelen, P.J. 2000. Estimation of areal soil water content through microwave remote sensing. Ph.D. thesis. Wageningen University, The Netherlands.

van Overmeeren, R.A., S.V. Sariowan, and J.C. Gehrels. 1997. Ground penetrating radar for determining volumetric soil water content; results of comparative measurements at two sites. J. Hydrol. (Amsterdam) 197:316–338.

Vasco, D.W., J.E. Peterson, and K.H. Lee. 1997. Ground-penetrating radar velocity tomography in heterogeneous and anisotropic media. Geophysics 62:1758–1773.

Vellidis, G., M.C. Smith, D.L. Thomas, and L.E. Asmussen. 1990. Detecting wetting front movement in a sandy soil with ground-penetrating radar. Trans. ASAE 33:1867–1874.

Weiler, K.W., T.S. Steenhuis, J. Boll, and K.-J.S. Kung. 1998. Comparison of ground penetrating radar and time domain reflectometry as soil water sensors. Soil Sci. Soc. of Am. J. 62:1237–1239.

West, L.J., K. Handley, Y. Huang, and M. Pokar. 2003. Radar frequency dielectric dispersion in sandstone: Implications for determination of moisture and clay content. Water Resour. Res. 39. DOI:10.1029/2001WR000923.

Wyseure, G.C.L., M.A. Mojid, and M.A. Malik. 1997. Measurement of volumetric water content by TDR in saline soils. Eur. J. Soil Sci. 48:347–354.

Yilmaz, O. 1987. Seismic data processing. SEG Investigations in Geophysics 2. Society of Exploration Geophysicists, Tulsa, OK.

Zhou, C., L. Liu, and J.W. Lane. 2001. Nonlinear inversion of borehole-radar tomography data to reconstruct velocity and attenuation distribution in earth materials. J. Appl. Geophys. 47:271–284.